

PAPER • OPEN ACCESS

## Red Dwarfs as Sources of Cosmic Rays and First Detection of TeV Gamma-rays from these stars

To cite this article: V.G. Sinitysna *et al* 2019 *J. Phys.: Conf. Ser.* **1181** 012018

View the [article online](#) for updates and enhancements.

You may also like

- [Implications of current nuclear cross sections on secondary cosmic rays with the upcoming DRAGON2 code](#)  
P. De La Torre Luque, M.N. Mazziotta, F. Loparco et al.
- [Chapter 4 Cosmic-Ray Physics](#)  
Benedetto D'Ettorre Piazzoli, Si-Ming Liu, et al.
- [Anisotropies of different mass compositions of cosmic rays](#)  
Bing-Qiang Qiao, Wei Liu, Yi-Qing Guo et al.



**ECS**  
The  
Electrochemical  
Society  
Advancing solid state &  
electrochemical science & technology

**DISCOVER**  
how sustainability  
intersects with  
electrochemistry & solid  
state science research

# Red Dwarfs as Sources of Cosmic Rays and First Detection of TeV Gamma-rays from these stars

V.G. Sinitysna, V.Y. Sinitsyna, Yu.I. Stozhkov

P.N. Lebedev Physical Institute, RAS, Moscow, Leninsky pr. 53

e-mail: sinits@sci.lebedev.ru, stozhkov@sci.lebedev.ru

**Abstract.** Conventional sources of Galactic cosmic rays are believed to be supernovae and supernova remnants that are powerful enough to accelerate particles up to  $10^{17}$  eV. Meanwhile, an interpretation of recent experimental data obtained by PAMELA, Fermi-LAT, and AMS-02 spectrometers hints at a possibility that some cosmic-ray sources may be located in a close proximity of the solar system, at the distances less than 1 kpc. Presence of such local sources could explain the unexpected raise of the positron fraction in cosmic rays, complex shapes of the proton and helium spectra, and even anomalous low-energy cosmic rays. We consider active dwarf stars as possible sources of Galactic cosmic rays in the energy range up to  $10^{14}$  eV. These stars are producing powerful stellar flares. Meanwhile, generation of high-energy cosmic rays should be accompanied by the high-energy  $\gamma$ -ray emission, which may be observed. Here we present the results of the SHALON long-term observations aimed to search for  $\gamma$ -ray emission above 800 GeV from the active red dwarf stars.

## 1. Introduction

Conventional sources of cosmic rays are believed to be supernovae and supernova remnants (SNRs) that can accelerate particles up to  $\sim 10^{17}$  eV. Indeed, because of their energetics SNRs could operate as powerful accelerators of cosmic-ray particles [1, 2]; this idea was prevailing from the very beginning of the cosmic-ray era. Recent observations of several SNRs in X-rays and TeV  $\gamma$ -rays reveal clear signatures of accelerated particles in their shells (see [3] and references within). The presence of relativistic electrons is clearly seen across the whole electromagnetic spectrum, from radio to very high-energy  $\gamma$ -rays, while signatures of accelerated protons can be only detected in high energy  $\gamma$ -rays. However, an interpretation of recent observations by PAMELA, Fermi-LAT, and AMS-02 hints at a possible presence of nearby sources of cosmic rays at the distances less than 1 kpc from the solar system. In particular, presence of such sources could explain the unexpected raise of the positron fraction in cosmic rays (Fig. 1) [4 – 7]. Such sources may also help with interpretation of the complex spectral behavior of protons, helium, and other species [8 – 10], and the appearance of the anomaly low-energy component (single ionized atoms) in cosmic rays. If the nearby cosmic-ray sources exist indeed, they could also generate high-energy  $\gamma$ -ray emission and may be observable with  $\gamma$ -ray telescopes.

The SHALON instrument [3, 11 – 15] consists of two imaging atmospheric Cherenkov telescopes located in Tien-Shan mountains at an altitude of 3340 m above the sea level. It is designed for observations of  $\gamma$ -ray sources in the energy range from 800 GeV to 100 TeV. Each of the telescopes has a composite mirror with an area of  $11.2 \text{ m}^2$ . The detector has the largest field of view  $>8^\circ$  among similar instruments. It allows the background from charged cosmic-ray particles and the atmospheric



transparency to be continuously monitored simultaneously with the observations of  $\gamma$ -ray sources. The SHALON method of selection of  $\gamma$ -ray showers from the background cosmic-ray showers allows the rejection of 99.93% of the background events. The minimum detectable integral flux of  $\gamma$ -rays at 1 TeV is  $2.1 \times 10^{-13} \text{ cm}^{-2} \text{ s}^{-1}$ . In the energy range from 1 – 50 TeV the minimum detectable flux falls to the value of  $6 \times 10^{-14} \text{ cm}^{-2} \text{ s}^{-1}$  [3, 12 – 14]. The SHALON experiment has been in operation since 1992 providing the long-term observations of many different types of sources that are of interest for many areas of astroparticle physics. One of the goals of the SHALON long-term observational program is to search for  $\gamma$ -ray emission above 800 GeV from the active red dwarf stars.

In this paper we study the active dwarf stars that produce powerful stellar flares and may accelerate cosmic-ray species up to  $10^{14}$  eV. Generation of high-energy cosmic rays in their flares should be accompanied by the high-energy  $\gamma$ -ray emission. Here we present the results of 10 – 20 years of observations of the dwarf stars V962 Tau, V780 Tau, V388 Cas, and V1589 Cyg with the SHALON atmospheric Cherenkov telescope.

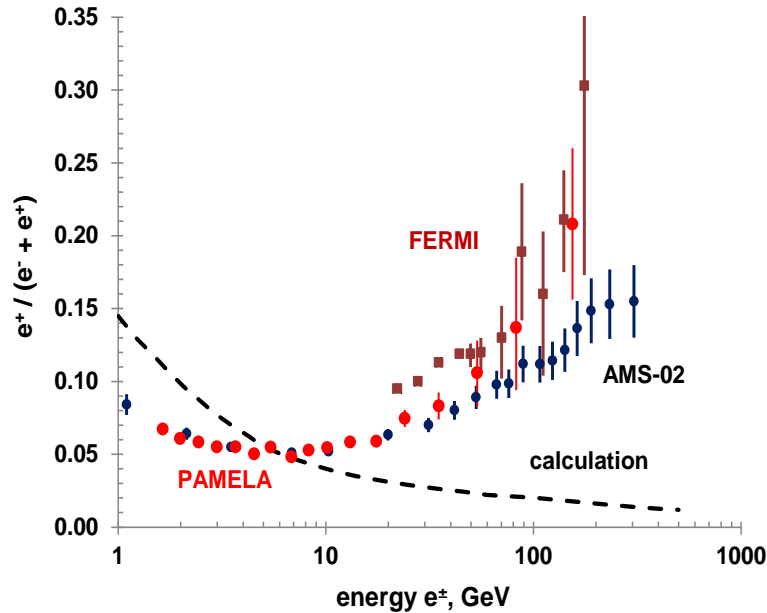


**Figure 1.** The positron fraction as measured by PAMELA, AMS, Fermi-LAT [4 - 6] together with theoretical predictions [16] (dashed line).

## 2. Observations of red dwarfs

As it was shown in the dedicated studies, the flare frequency of the active red dwarf stars is uncertain [17, 18], and their observations require a long-term monitoring program. In this study we present our results for those stars that we observed over very extended periods of time.

In accordance with the long-term program of observations of the Galactic  $\gamma$ -ray sources, more than ten-years long observations of the Tycho's SNR, Crab Nebula, and Cyg X-3 have been carried out by the SHALON experiment [3, 11 – 14]. During these pointed observations, some of the red dwarfs were also observed by SHALON as they are located at the angular distances less than  $\sim 5^\circ$  from those well-known TeV  $\gamma$ -ray sources while the field of view of the instrument is  $> 8^\circ$ . The observations and data processing were performed using the standard SHALON technique [3, 13].

### 2.1. V388 Cas

Tycho's SNR was observed by SHALON during the 123 hours from 1996 to 2010 [3, 14, 15]. All observations were made during moonless nights with zenith angles from  $16^\circ$  to  $35^\circ$ . During Tycho's SNR observations the SHALON field of view also included V388 Cas located  $\sim 4.5^\circ$  south of Tycho's

SNR. V388 Cas is a UV Cet type star at a distance of  $\sim 10$  pc [19]. It is also present in the ROSAT catalogue with the photon flux of  $\sim 1.7 \times 10^{-12} \text{ erg cm}^{-2} \text{ s}^{-1}$  and luminosity of  $10^{28.3} \text{ erg s}^{-1}$  [19]. V388 Cas was observed by SHALON for a total of 93 hours from 1996 to 2010. The  $\gamma$ -ray source associated with the V388 Cas was detected above 1 TeV with a statistical significance of  $6.8\sigma$  determined according to Li and Ma [20] method with an average  $\gamma$ -ray flux of  $I_{\text{V388Cas}}(> 1\text{TeV}) = (0.84 \pm 0.21) \times 10^{-12} \text{ cm}^{-2} \text{ s}^{-1}$ .

The signal significance of this source is much less than that of the source with a similar flux and the spectral index obtained during the same hours of observations because of the smaller collection area of the instrument relative to the standard procedure of the SHALON experiment. After processing of the Tycho's SNR observational data, first using the selection criteria associated with Tycho's SNR and then with V388 Cas, we found that less than 1% of showers were common for both sources. Recognition of the source of each of the common showers was performed through the analysis of the angular distance of the arrival directions of these showers and the source positions. This procedure does not change the average flux of Tycho's SNR. The shape of the SHALON average differential spectrum of V388 Cas (Figs. 2, 4) in the energy range from 0.8 to 25 TeV can be fitted with a soft power law:  $dN/dE = (0.91 \pm 0.25) \times 10^{-12} \times (E_\gamma/1\text{TeV})^{-2.52 \pm 0.15} \text{ TeV}^{-1} \text{ cm}^{-2} \text{ s}^{-1}$  with  $\chi^2/\text{Dof} = 1.23$ , where the number of the degrees of freedom  $\text{Dof} = 6$ . During the long-term observations, V388 Cas was detected as a variable source that was visible during the flares. Its flaring spectrum,  $dN/dE_{\text{Flare}} = (2.7 \pm 0.15) \times 10^{-12} \times (E_\gamma/1\text{TeV})^{-2.91 \pm 0.18} \text{ TeV}^{-1} \text{ cm}^{-2} \text{ s}^{-1}$ , is shown in Fig. 2 ( $\blacktriangle$ ). The integral flux of V388 Cas averaged over a one-year interval is shown in Fig. 4. As it is clearly seen in Fig. 4 that V388 Cas has been detected during the flares that occurred before 2008 and that resulted in high fluxes presented in Fig. 2.

Searching for counterparts in the Fermi-LAT 8 years catalogue (FL8Y), we found an unassociated source J0106.4+5938 [21] of high energy emission that is located at a distance of  $\sim 2.5^\circ$  from V388 Cas. The FL8Y source catalogue is based on the data taken during the period from 2008 August 4 to 2016 August 2. The emission from J0106.4+5938 was detected by Fermi LAT at the level of  $4.2\sigma$  significance in the energy range from 100 MeV to 1 TeV. The shape of differential photon spectrum in the energy range from 100 MeV to 100 GeV is fitted with a power law  $dN/dE = C(E/0.913\text{GeV})^{-\Gamma}$ , where  $\Gamma = 2.78 \pm 0.16$  and  $C = (5.8 \pm 1.2) \times 10^{-13} \text{ MeV}^{-1} \text{ cm}^{-2} \text{ s}^{-1}$ .

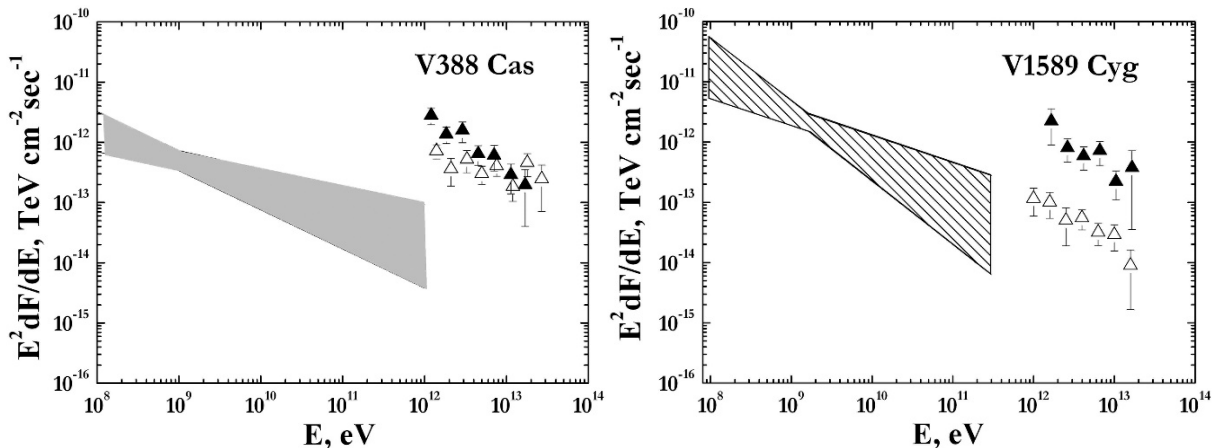


**Figure 2.** Spectral energy distributions of V388 Cas (left) and V1589 Cyg (right). Open and black triangles ( $\triangle$ ,  $\blacktriangle$ ) show SHALON data from long-term observations (see text). The grey bow tie on V388 Cas plot indicates the minimum flux needed for a Fermi LAT  $5\sigma$  detection of a soft-spectrum point source [22, 23]. The spectrum of the unassociated source J2041.2+41.76 observed from FL8Y is shown with a bow tie (right).

## 2.2. V1589 Cyg

The Cygnus Region was observed by SHALON in the framework of the long-term studies of microquasar Cyg X-3 at very high energies. Observations also included such sources as V1589 Cyg, TeV J2032+4130, and  $\gamma$ Cygni SNR – thanks to the large field of view of SHALON [12 – 14, 24, 25]. V1589 Cyg is an M-class flaring star located at a distance of 23-32 pc [17]. Its luminosity is significantly fluctuating with duration of flares from minutes to hours [17].

V1589 Cyg is located  $\sim 2^\circ$  west of Cyg X-3. Consequently, V1589 Cyg has been systematically observed by the SHALON telescope in 1995 – 2016 during clear moonless nights at zenith angles from  $5^\circ$  to  $34^\circ$  for a total of 303.5 hours. V1589 Cyg was detected by SHALON above 0.8 TeV with the average integral flux of  $I_{V1589Cyg}(> 0.8\text{TeV}) = (0.13 \pm 0.019) \times 10^{-12} \text{ cm}^{-2} \text{ s}^{-1}$ . The statistical significance of the detection is  $6.5\sigma$  [20]. As with observations of V388 Cas dwarf star, we found that less than 1% of Cyg X-3 showers were identified to be V1589 Cyg showers. This did not change the average flux of Cyg X-3. During the long-term observations V1589 Cyg appeared as a source with a highly variable flux. The flaring spectrum was also extracted and presented in Fig. 2 ( $\blacktriangle$ ). The spectral shape of V1589 Cyg in the energy range from 0.8 to 35 TeV can be fitted with a soft power law (see Fig. 2,  $\triangle$ ),  $dN/dE = (0.15 \pm 0.05) \times 10^{-12} (E_\gamma/1 \text{ TeV})^{-2.91 \pm 0.18} \text{ TeV}^{-1} \text{ cm}^{-2} \text{ s}^{-1}$  with the  $\chi^2/\text{Dof} = 0.89$ , where  $\text{Dof} = 5$ . A flaring spectrum is  $dN/dE_{\text{Flare}} = (1.7 \pm 0.45) \times 10^{-12} (E_\gamma/1 \text{ TeV})^{-3.15 \pm 0.29} \text{ TeV}^{-1} \text{ cm}^{-2} \text{ s}^{-1}$ . The light curve of V1589 Cyg during the observations from 1995 to 2016 is presented in Fig. 4, where the individual points are the integral fluxes averaged over each year of observations.

An unassociated object FL8Y J2041.2+41.76 [21] was detected by Fermi-LAT at a distance of  $\sim 0.45^\circ$  from V1589 Cyg. The high energy emission was detected at the level of  $5.6\sigma$  significance. The differential photon spectrum was obtained in the energy range from 100 MeV to 100 GeV. The spectrum was fitted with a power law  $dN/dE = C(E/1.63\text{GeV})^{-\Gamma}$ , where  $\Gamma = 2.82 \pm 0.26$  and  $C = (7.63 \pm 1.3) \times 10^{-13} \text{ MeV}^{-1} \text{ cm}^{-2} \text{ s}^{-1}$  (see Fig. 2, right). The FL8Y spectrum of J2041.2+41.76 is consistent with SHALON observations of V1589 Cyg at TeV energies.

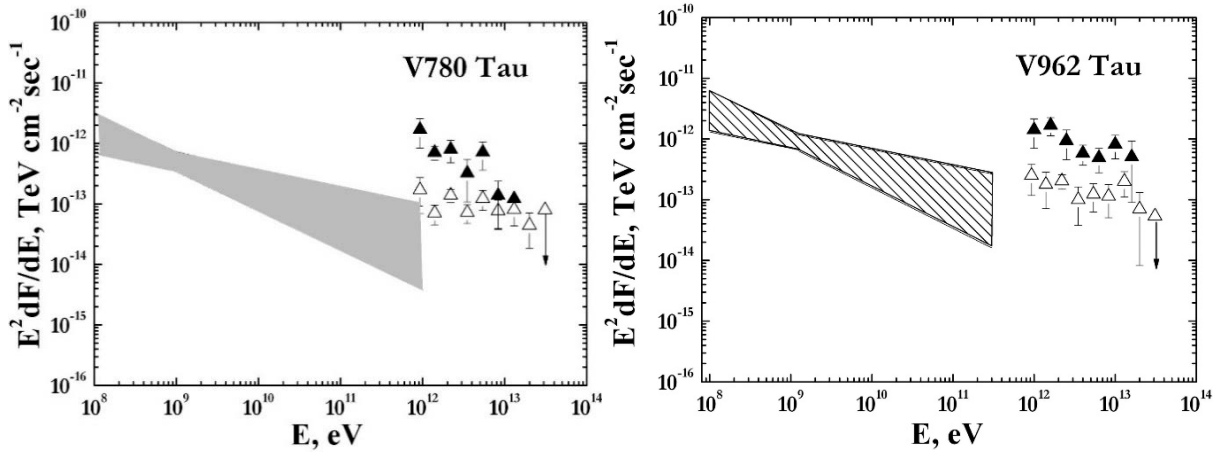


**Figure 3.** Spectral energy distributions of V780 Tau (left) and V962 Tau (right). Open and black triangles ( $\triangle$ ,  $\blacktriangle$ ) show SHALON data from long-term observations (see text). The grey bow tie on V780 Tau plot indicates the minimum flux needed for the integral  $5\sigma$  detection of point source with soft spectrum by Fermi LAT [22, 23]. The  $\gamma$ -ray spectrum of the unassociated source J0544.7+2239 from FL8Y is shown with a bow tie (right).

### 2.3. V962 Tau and V780 Tau

SHALON observations of the Crab Nebula also yielded observations of two flaring stars: V962 Tau and V780 Tau. V962 Tau and V780 Tau are the flaring type of UV Cet type with the spectrum of the red star class [19, 26] at distances of about 10 pc. V780 Tau was also observed by ROSAT with the flux of  $\sim 3.6 \times 10^{-13} \text{ erg cm}^{-2} \text{ s}^{-1}$  and the luminosity of  $10^{27.6} \text{ erg s}^{-1}$  [19].

V780 Tau is located  $\sim 3^\circ$  north of Crab and V962 Tau is  $\sim 2.5^\circ$  east of Crab. These stars have a separation of  $\sim 4^\circ$ . Consequently, both stars were observed by the SHALON telescope from 1994 to

2014 [11, 25] for a total of 125.2 hours during clear moonless nights at zenith angles from  $15^\circ$  to  $35^\circ$ . V780 Tau and V962 Tau were detected by SHALON above 0.8 TeV with the average integral fluxes:  $I_{V780\text{Tau}}(>1 \text{ TeV}) = (0.23 \pm 0.03) \times 10^{-12} \text{ cm}^{-2} \text{ s}^{-1}$  and  $I_{V962\text{Tau}}(>1 \text{ TeV}) = (0.39 \pm 0.04) \times 10^{-12} \text{ cm}^{-2} \text{ s}^{-1}$ , correspondingly.

V780 Tau was detected with a statistical significance  $6.1\sigma$  [20]. Again, in this case we found that less than 1% of showers are common for the Crab Nebula and V780 Tau. Identification of the source of each of the common showers was performed through the analysis of the angular distances of the arrival directions of these showers and the source positions. As the result, less than  $\sim 0.4\%$  of the Crab showers were identified to be V780 Tau showers. This did not change the average flux of Crab. The differential spectrum of V780 Tau in the energy range from 0.8 to 20 TeV can be fitted with a power law:  $dN/dE = (0.21 \pm 0.08) \times 10^{-12} \times (E_\gamma/1 \text{ TeV})^{-2.51 \pm 0.15} \text{ TeV}^{-1} \text{ cm}^{-2} \text{ s}^{-1}$  with the  $\chi^2/\text{Dof} = 1.31$ , where  $\text{Dof}=5$  (Fig. 3,  $\triangle$ ). Its flaring spectrum is  $dN/dE_{\text{Flare}} = (2.0 \pm 0.15) \times 10^{-12} \times (E_\gamma/1 \text{ TeV})^{-3.01 \pm 0.21} \text{ TeV}^{-1} \text{ cm}^{-2} \text{ s}^{-1}$  (Fig. 3,  $\blacktriangle$ ). As can be seen on Fig. 4, V780 Tau was not active since 2008.

An unassociated object FL8Y J0540.5+2305 [21] is located at a distance of  $\sim 1.6^\circ$  from V780 Tau. The emission from the unassociated source was detected by Fermi LAT at the level of  $6.62\sigma$  significance in the energy range from 100 MeV to 1 TeV. The differential photon spectrum in the energy range from 100 MeV to 100 GeV was fitted with a power law  $dN/dE = C(E/1.034 \text{ GeV})^{-\Gamma}$ , where  $\Gamma = 2.8 \pm 0.13$  and  $C = (1.84 \pm 0.23) \times 10^{-12} \text{ MeV}^{-1} \text{ cm}^{-2} \text{ s}^{-1}$ .

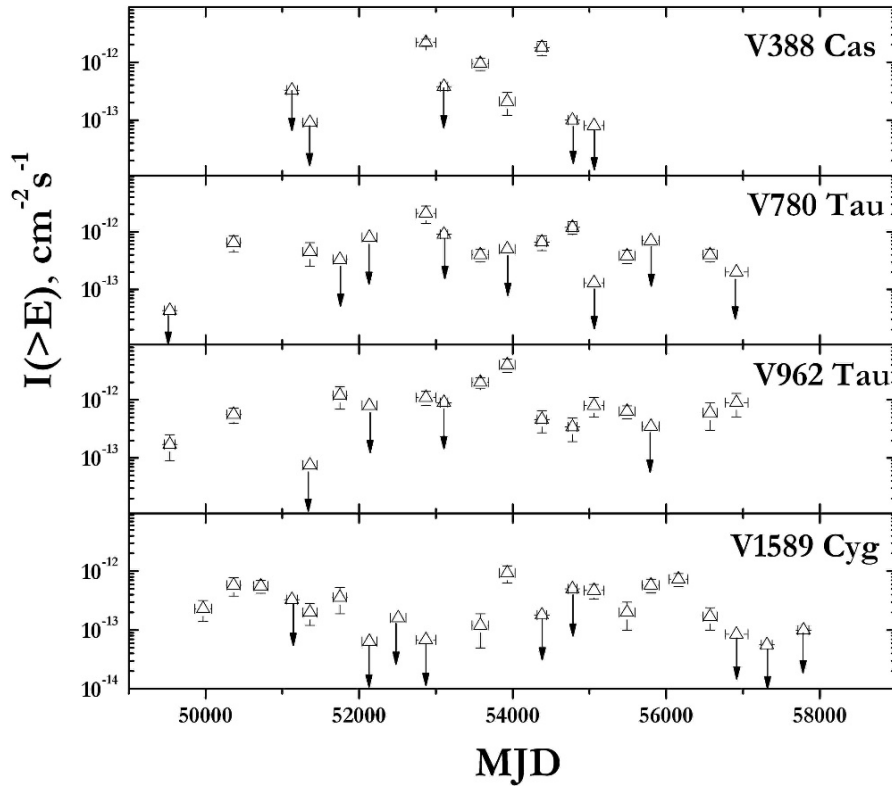


**Figure 4.** Light curves of V388 Cas, V780 Tau, V962 Tau and V1589 Cyg at TeV energies obtained in the long-term SHALON observations.

V962 Tau was detected by SHALON above 0.8 TeV with a statistical significance  $7.7\sigma$  [20]. Here we found that there are no showers common for the Crab Nebula and V962 Tau. V962 Tau was also found to be variable. The differential spectrum of  $\gamma$ -ray emission from V962 Tau in the energy range from 0.8 to 20 TeV can be fitted with a power law:  $dN/dE = (0.40 \pm 0.17) \times 10^{-12} \times (E_\gamma/1 \text{ TeV})^{-2.54 \pm 0.15} \text{ TeV}^{-1} \text{ cm}^{-2} \text{ s}^{-1}$  with the  $\chi^2/\text{Dof} = 0.87$ , where  $\text{Dof}=6$  (Fig. 2,  $\triangle$ ). The flaring spectrum is  $dN/dE_{\text{Flare}} = (2.8 \pm 0.45) \times 10^{-12} (E_\gamma/1 \text{ TeV})^{-2.95 \pm 0.22} \text{ TeV}^{-1} \text{ cm}^{-2} \text{ s}^{-1}$  (Fig. 3,  $\blacktriangle$ ).

Both these active red dwarfs, V780 Tau and V962 Tau, are displaying variable fluxes at TeV energies. In Fig. 4 we present the light curves of V780 Tau and V962 Tau obtained during the long-term observations.

The emission from unassociated source 3FGL J0544.7+2239 [27] at the distance of  $\sim 0.33^\circ$  from V962 Tau was detected by Fermi LAT in the energy range 100 MeV – 300 GeV with significance of  $4.24\sigma$ . The Fermi-LAT spectrum was fitted with a power law  $dN/dE = C(E/1.26 \text{ GeV})^{-\Gamma}$ , where  $\Gamma = 2.49 \pm 0.18$  and  $C = (5.1 \pm 1.1) \times 10^{-13} \text{ MeV}^{-1} \text{ cm}^{-2} \text{ s}^{-1}$  (Fig. 3). The Fermi-LAT spectrum of this unassociated source is consistent with the SHALON spectrum of V962 Tau at TeV energies.

### 3. Discussion

During the long-term observations, red dwarfs appear as sources with variable TeV  $\gamma$ -ray flux up to  $\sim 10$  TeV and seems are detected mostly during the flares. The observed light curves of V388 Cas, V780 Tau, V962 Tau and V1589 Cyg at TeV energies are shown in Fig. 4, where we show the integral fluxes averaged over a one-year interval. M-Dwarf stars are characterized by flaring events which occur frequently with different flare duration [17, 18]. Very high energy  $\gamma$ -ray fluxes presented here demonstrate that these objects produce flares with total energy of  $\sim 10^{33} - 10^{35}$  ergs.

High energy emission from unassociated sources in the vicinity of V1589 Cyg and V962 Tau red dwarfs was detected by Fermi-LAT. Spectral energy distributions of these objects are shown in Figs. 2, 3. The red dwarfs are flaring stars with uncertain frequency and duration of the flares. Unfortunately, V388 Cas and V780 Tau were not active enough after 2008 to produce a significant detection by Fermi-LAT launched in 2008 (see Fig. 4). In contrast, V1589 Cyg and V962 Tau were quite active during the whole period of observations and the unassociated sources nearby detected by Fermi-LAT may actually be these red dwarfs.

The so-called positron excess, or unexpected raise of the positron fraction, was discovered by the PAMELA experiment and then confirmed by Fermi-LAT and AMS-02, while this fraction is expected to decrease [16]. The observed positron fraction is starting to increase at  $\sim 5$  GeV and then goes up monotonically up to  $\sim 350$  GeV. A possible interpretation of this effect may involve the active dwarf stars [7] as the sources of cosmic rays up to  $\sim 10^{14}$  eV.

Indeed, the stellar flares of active dwarf stars could effectively accelerate cosmic rays and compete with other sources. Among the huge variety of stars in our Galaxy, in which there are  $\sim 2 \times 10^{11}$  stars in total, more than 95% are dwarf stars of G-M spectral classes [19]. Assuming that 10% of the dwarf stars in our Galaxy produce stellar flares with frequency of flares of about  $36 \text{ year}^{-1}$  and average energy released in a single flare of about  $10^{35}$  ergs, one can find that their total energy is  $\sim 1.4 \times 10^{54}$  erg which is comparable to the conventional estimates of the total energy of Galactic cosmic rays in the Galactic disk  $W_{\text{GCR}} \sim 2 \times 10^{54}$  erg [7].

During powerful flares of active dwarf stars, high-energy protons are generated with a maximum energy of  $E < 10^{14}$  eV. Some of these accelerated protons could escape into the interstellar medium. Others enter the photosphere of the star and undergo nuclear interactions with its matter. During these interactions,  $\pi^0$  and  $\pi^\pm$  are produced, while positrons and electrons are produced through the  $\pi^\pm$  to  $\mu^\pm e^\pm$  decay. An additional source of positrons is the decay of neutral pions into two  $\gamma$ -rays and the subsequent formation of  $(e^+e^-)$  pairs by these  $\gamma$ -rays. Such a process is observed during the large solar flares (the Sun is a yellow dwarf). Positrons and electrons from stellar flares with  $E > 5$  GeV escape into the interstellar medium from a flare region with strong magnetic fields. If the energy of these particles  $E < 5$  GeV they have no chance to escape from the flare region, but if their energy is  $> 100$  GeV they escape from the flare region with a high probability ( $\sim 100\%$ ). In the intermediate energy interval  $5 < E < 100$  GeV the probability of particle escape increases with energy. It is thus possible to obtain an increase in the positron fraction similar to the data plotted in Fig. 1. It should be noted that mainly electrons (and protons) are accelerated during the stellar flares, meanwhile an addition of this another component to the electron cosmic-ray flux constitutes only a small fraction of the total flux. This additional source of positrons, however, provides an essential addition to the flux of these particles up to energies of  $E \sim 500$  GeV. Estimates show that the mechanism suggested in [7] could

explain the observed increase in the positron fraction above  $\sim 5$  GeV. According to the observations, the positron flux increases from 5 GeV up to  $\sim 100$  GeV and then becomes about a constant in the energy range from 200 – 350 GeV (see Fig. 1). What could we expect in the energy range above 350 GeV? According to the scenario suggested in [7] the positron fraction has to decrease to the values calculated in [16] because the highest energy of accelerated particles in the stellar flares is unlikely to exceed  $10^{14}$  eV.

#### 4. Conclusion

The results of long-term observations of M-Dwarf stars V388 Cas, V780 Tau, V962 Tau and V1589 Cyg by the SHALON atmospheric Cherenkov telescope are presented. Very high energy  $\gamma$ -ray emission from these sources is detected in the range of 1 - 10 TeV mostly during the flaring states. The emission is characterized by a soft power-law spectrum with index of  $\sim 2.6 \div 3.2$ . The high energy emission from nearby unassociated sources detected by Fermi LAT may be originated in red dwarfs. This result confirms that active dwarf stars are also the sources of high energy cosmic rays. Estimates [7] show that such sources could explain the raise of the positron fraction observed with PAMELA, Fermi-LAT, and AMS spectrometers.

#### References

- [1] Berezhko E G and Krymskii G F 1988 Usp. Fiz. Nauk **154**(1) 49
- [2] Reynolds S P 2008 Ann. Rev. Astron. Astrophys. **46** 89
- [3] Sinitsyna V G, Sinitsyna V Yu et al. 2018 Advances in Space Research **62**(10) 2845
- [4] Adriani O, Barbarino G C, Bazilevskaya G A, et al. 2009 Nature. **458** No 7238 607
- [5] Ackermann M, et al. 2012 Phys. Rev. Lett. **108**, 011103
- [6] Aguilar M, Alberti G, Alpat B, et al. 2013 Phys. Rev. Lett. **110** 141102
- [7] Stozhkov Yu I 2011 Bull. of RAS, ser. Physics **75**(3) 323
- [8] Aguilar M, Cavasonza L Ali, Alpat B et al, 2017 Phys. Rev. Lett. **119** 251101
- [9] Aguilar M, Cavasonza L Ali, Ambrosi G et al 2018 Phys. Rev. Lett. **120** 021101
- [10] Aguilar M, Cavasonza L Ali, Alpat B et al 2018 Phys. Rev. Lett. **121** 051103
- [11] Sinitsyna V G 1996 Nuovo Cim. **19C** 965
- [12] Sinitsyna V G 1998 Proc. of the 16th European Cosmic Ray Symposium, ed J Medina (Univ. de Alcala, Alcala de Henares, Spain) p 383
- [13] Sinitsyna V G and Sinitsyna V Yu 2018 Astron. Lett. **44**(3) 162
- [14] Sinitsyna V G 1997 Towards a Major Atmospheric Cherenkov Detector-V, (Kruger Park) ed O C deJager (Potchefstroom: Westprint) p 136, 190
- [15] Sinitsyna V G and Sinitsyna V Yu 2011 Astron. Lett. **37**(9) 621
- [16] Moskalenko I V and Strong A W, 1998 Astrophys. J., **493** 694
- [17] Pettersen B R, Tsvetkov M K, Hawley S L et al., 1988 Astrophysics **29**(1) 67
- [18] Ohm S and Hoischen C 2018 MNRAS **474** 1335
- [19] Gershberg R E et al., 1999 Astron. Astrophys. Suppl. Ser. **139** 555
- [20] Li T-P and Ma Y-Q, 1983 Astrophys. J. **272** 317
- [21] <https://fermi.gsfc.nasa.gov/ssc/data/access/lat/fl8y/>
- [22] [http://www.slac.stanford.edu/exp/glast/groups/canda/lat\\_Performance.htm](http://www.slac.stanford.edu/exp/glast/groups/canda/lat_Performance.htm)
- [23] [https://fermi.gsfc.nasa.gov/ssc/data/analysis/documentation/Cicerone/Cicerone\\_LAT\\_IRFs/LAT\\_sensitivity.html](https://fermi.gsfc.nasa.gov/ssc/data/analysis/documentation/Cicerone/Cicerone_LAT_IRFs/LAT_sensitivity.html)
- [24] Sinitsyna V G, Sinitsyna V Y 2013 Bull. of the Lebedev Physics Institute (New York: Allerton Press, Inc.), **40**(5) 113
- [25] Sinitsyna V G et al., 2016, J. Phys.: Conf. Ser. **718** 052045
- [26] Hatsunzev I V 1986 Variable Stars **22**(3) 431
- [27] [https://fermi.gsfc.nasa.gov/ssc/data/access/lat/4yr\\_catalog/](https://fermi.gsfc.nasa.gov/ssc/data/access/lat/4yr_catalog/)